PLL-less Robust Active and Reactive Power Controller for Single Phase Grid-Connected Inverter with LCL Filter

Xiao Li[1], *Student Member, IEEE* and Robert S. Balog[2], *Senior Member, IEEE*
Renewable Energy & Advanced Power Electronics Research Laboratory
Department of Electrical & Computer Engineering, Texas A&M University
College Station, Texas, 77843, USA
[1]xiaoli.tamu@gmail.com, [2]robert.balog@ieee.org

***Abstract*—Grid connected inverters, especially those used in DG (Distributed Generation) system, are expected with decoupled and flexible power control ability. Many existing power control methods are based on synchronous reference frame transformation, which requires the phase angle information provided by Phase-Locked Loop (PLL). This creates additional drawbacks of the system and makes the system complex. This paper presents a controller for single-phase grid connected inverter system with LCL filter in stationary reference frame. And PLL is avoided. Compared with traditional power control scheme for single phase grid-connected inverter controller, this control scheme has faster response, higher reliability and decoupled real and reactive power control ability. Moreover, the proposed controller has good robustness under different distorted grid conditions. Since the controller is totally implemented in stationary reference frame, the control algorithm comes to be simpler and easier. The designed current controller, combining the active damping technique, helps restrain the high resonant peak value. Compared with traditional PI based current controller, the designed current controller, which is based on the Proportional & Resonant (PR) controller, provides the system with high gain in wide range of frequency to track given reference value fast and output excellent grid current with low THD.**

Keywords—single-phase inverter; grid-connected; Phase-Lock Loop; LCL filter; active damping; decoupled power control; PR controller; grid distortion

I. INTRODUCTION

Many power control strategies for the single-phase inverter have been proposed [1-4]. Generally, synchronous reference transformation and decoupling algorithms are used in the control process, which complexes the control algorithm [5-7]. And this requires the amplitude and phase angle information of the AC mains voltage captured by the PLL. However, the PLL module, as a nonlinear part, usually degrades the output performance of system. And much effort is needed to design the parameters in PLL to get the desired performance, which increases the complexity and cost of design.

Moreover, due to the nature of weak grid, the grid voltage may have various disturbances such as sag, swell, frequency distortion, and contamination with voltage harmonics. The disturbances in grid can degrade the performance of PLL largely [8]. In the proposed controller, the synchronization function is embedded into the power controller. In this way, the PLL unit is not required, so the complexity for designing the system can be decreased. Meanwhile, the proposed system keeps good performance of decoupled real and reactive power control with excellent grid current quality under different conditions of grid disturbance.

Inverter system with LCL filter is a high order system and has high resonant peak value. To overcome the promising resonance problem, active damping technique with double-loop current control is applied into the controller design of this system. Traditional grid current controller for single phase inverter with LCL filter is based on PI controller, which is not able to follow a sinusoidal reference without steady state error due to the dynamics of the integral term. And its current tracking performance will be worse under non-ideal grid condition. Though this can be resolved by feedforward control of grid voltage to some extent, this can increase the complexity of system. In the designed inner current loop, Proportional & Resonant (PR) controller is used to provide the system with rapid response and high gain in wide range of frequency.

In this paper, we will analyze and evaluate the proposed controller for single-phase grid connected inverter with LCL filter. Reliable performance under various grid distortion cases, high-quality output current and decoupled real and reactive power control abilities of inverter system are achieved in this way. Both simulation and experiment results show the effectiveness of the proposed controller.

II. GRID-CONNECTED INVERTER

Fig. 1 shows the topology of an LCL-filter-based grid-connected inverter. The DC bus could be supplied by renewable energy resources, such as photovoltaic, wind generator, storage battery, super capacitor, etc. The inverter is used to convert electricity energy from DC to AC and could be bi-directional. The LCL filter restrains the high-frequency harmonics.

The relationships between V_s, V_g and I_2 in Fig. 1 can be expressed in (1). Fig. 2 shows the bode plot of the open-loop transfer function from V_o to I_2. Obviously, there exists a rather high resonant peak in the LCL filter, which is undesired for the control system design.

$$I_2 = V_O \frac{1}{L_1 L_2 C s^3 + (L_1 + L_2)s} - V_g \frac{L_1 C s^2 + 1}{L_1 L_2 C s^3 + (L_1 + L_2)s} \tag{1}$$

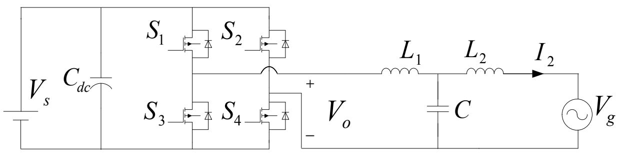

Fig. 1. Power stage of single-phase LCL-filter-based

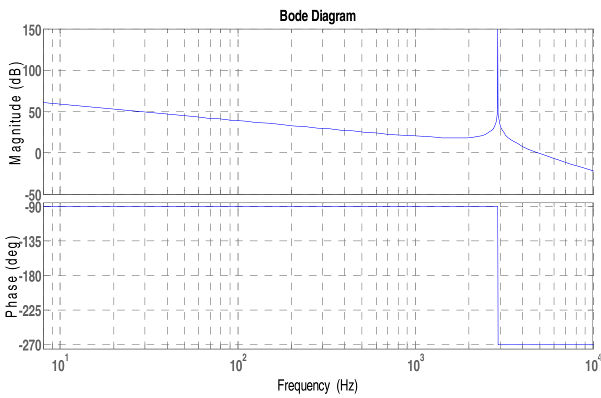

Fig. 2. Bode plots of the transfer function from V_o to I_2

III. CONTROLLER IN STATIONARY REFERENCE FRAME

Fig. 3 shows the structure of single-phase grid-connected inverter system with the proposed controller.

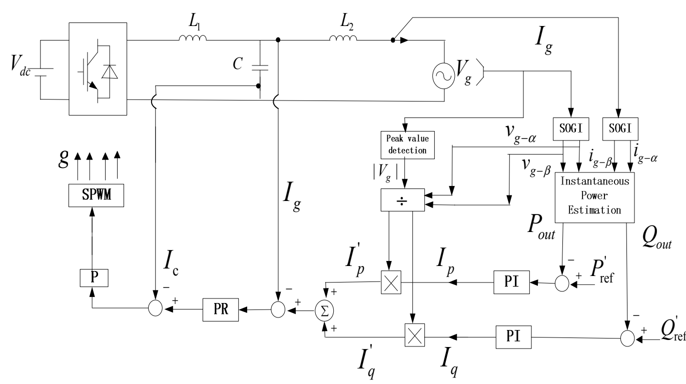

Fig.3. Control structure of proposed power control strategy

The grid-connected inverter is controlled with a multi-loop controller composed of a power outer loop and a current inner loop with active damping technique. The reactive power reference command is typically provided by the grid operator or user. This can be set to zero for unity, negative for leading, and positive for the lagging power factor. The active power reference is determined by the user or related with the instantaneous output power value supplied in the system, taking it as an example, for PV application, the active power reference should be the maximum power point determined from MPPT algorithm.

In the proposed controller, the instantaneous real power and reactive power values are calculated based on the instantaneous power theory. By comparing them with corresponding reference values, two independent control values, I_p and I_q, can be obtained. Then I_p and I_q are multiplied with two unit sinusoidal signals coming from the second order general integrator. In this way, two new signals, I'_p and I'_q, will be achieved and contain both angle and amplitude information, from which we can get the reference signal of grid current. In the proposed controller, the inner loop of the system is the current loop, whose main function is to improve the dynamic performance and ensure that the output current can track the reference well with low THD. Capacitor current feedback is also added into the current loop to overcome the resonance problem introduced by LCL filter.

A. Current Controller

Fig. 4 shows the block diagram of current controller.

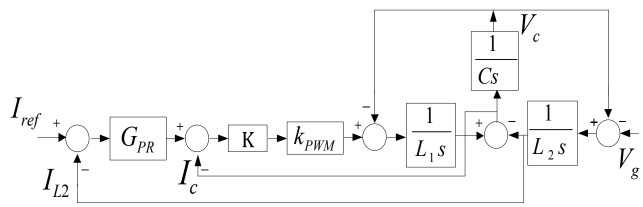

Fig. 4. Simplified block diagram of double loop control of current controller for LCL filter

The current reference value can be derived based on Fig. 3 as

$$I_{ref} = I'_p + I'_q = \frac{I_p V_{g-\alpha} + I_q V_{g-\beta}}{|V_g|} \tag{2}$$

Here, PR controller is applied to serve as the grid current loop compensator, which can provide infinite gain at the resonance frequency ω_0 to reach zero steady-state error. The transfer function of PR controller is given in (3). The corresponding bode plot is shown in Fig. 5.

$$G_s(s) = K_P + \frac{2K_R s}{s^2 + \omega_0^2} \tag{3}$$

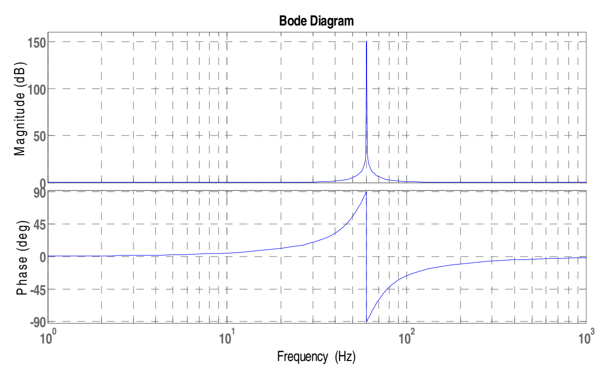

Fig.5. Bode plot of ideal PR controller with K_P=1,K_R=100

The dual closed loop current controller with capacitor current inner-loop and grid current outer-loop aims at current accuracy and acceptable distortion. The open-loop transfer function can be expressed as

$$G_o(s) = \frac{B_1 s^2 + B_2 s + B_3}{A_1 s^5 + A_2 s^4 + A_3 s^3 + A_4 s^2 + A_5 s} \quad (4)$$

Where, $B_1 = K_P K K_{PWM}$,

$B_2 = 2 K K_{PWM} K_R$,

$B_3 = K_P K K_{PWM} \omega_0^2$,

$A_1 = L_1 L_2 C$,

$A_2 = K K_{PWM} L_2 C$,

$A_3 = L_1 L_2 C \omega_0^2 + L_1 + L_2$,

$A_4 = L_2 C K K_{PWM} \omega_0^2$,

$A_5 = (L_1 + L_2)\omega_0^2$,

Based on the pole placement theory, the desired design parameters can be achieved. Here, to get the good dynamic performance of system, we choose K_P=3.3, K_R=3091.7.

B. Power Controller

After designing the current loop, the block diagram of power loop can be represented as Fig. 6, taking the control delay time into consideration. In this way, the bandwidth of outer loop should be less than that of inner loop.

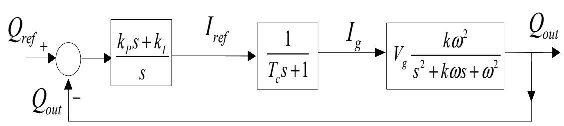

Fig.6. Block diagram of power loop

The open-loop transfer function of the power controller can be expressed as

$$G_0(s) = \frac{k_P s + k_I}{s} * V_g * \frac{k\omega^2}{s^2 + k\omega s + \omega^2} * \frac{1}{T_c s + 1} \quad (5)$$

Where, k_P and k_I is the parameters of PI controller; k and ω are two parameters of SOGI module, which will be introduced in detail in the following part. T_c is the control period of the whole system. It is very small in real implementation.

For the power outer loop, the main functions are to track the given power reference with zero steady-state error and ensure the stability of the system. Considering these control aims, the specific controller parameters can be determined with frequency response method.

Normally, V_g, the amplitude of grid voltage, will be a changeable variable in the distorted grid conditions. As can be seen in equation (5), V_g is also a variable that may affect the system performance. Here, due to the existence of SOGI module, which offering a high gain in the working frequency, the change of Vg will not affect the system's performance heavily in a certain frequency range. This can be proved in Fig. 7. When Vg changes from 250-350V, the system performance does not change a lot.

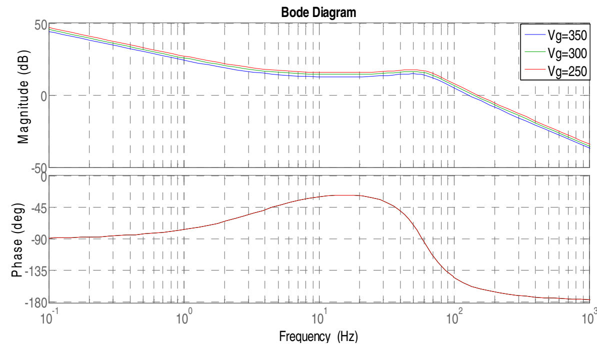

Fig.7. Bode plot of whole system when Vg amplitude change and power

(controller parameters keep as :k_P=0.02,k_I=0.5)

This characteristic can not only improve the reliability performance of system under distorted grid conditions, but also make it possible to apply the peak value detection method into the system. The peak value detection method is applied to get the maximum value of grid voltage, as shown in Fig. 3. The peak detection method can be implemented by taking the detected peak value in one or two cycles as the maximum value of grid voltage. Though this method may create error in the detection result, the detection error will not affect much on the performance of the whole system as mentioned above.

C. Second Order Generalized Integrator

To create an orthogonal signal from an original single-phase signal, different OSG techniques have been proposed in the literature. In the proposed controller, the second-order generalized integrator (SOGI)-based OSG is applied. This approach prevents harmonics/ noises from reaching the controller and therefore is suitable for this study. The input-to-output transfer function describing the dynamics of SOGI is shown in equations (6) and (7), where ω is the fundamental angular frequency.

$$\frac{x_\alpha(s)}{x(s)} = \frac{k\omega s}{s^2 + k\omega s + \omega^2} \quad (6)$$

$$\frac{x_\beta(s)}{x(s)} = \frac{k\omega^2}{s^2 + k\omega s + \omega^2} \quad (7)$$

The response of SOGI to the grid distortion is shown in Fig. 8.

In Fig. 8(a), ideal grid voltage (Vg=300V;fvg=60Hz) is designed to be combined with 8% 5^{th} ,8% 7^{th}, 8% 11^{th} harmonics. And it sags by 20% at time 0.07s and resume to original condition at time 0.17s. In Fig. 8(b), the frequency of ideal grid voltage changes from 60Hz to 58Hz at 0.07s. And it resume to original condition at time 0.17s.

From the above results, it can be seen that the SOGI module have a good performance in various distortion conditions, especially in grid harmonics distorted condition.

With the orthogonal signals created by SOGI modules, the instantaneous power values can be calculated based on instantaneous power theory. The corresponding calculation equations are shown in equations (8) and (9).

$$P = \frac{1}{2}(V_{g-\alpha} * I_{g-\alpha} + V_{g-\beta} * I_{g-\beta}) \tag{8}$$

$$Q = \frac{1}{2}(V_{g-\beta} * I_{g-\alpha} - V_{g-\alpha} * I_{g-\beta}) \tag{9}$$

Where, $V_{g-\alpha}, V_{g-\beta}$ are the derived orthogonal signals of grid voltage, and $I_{g-\alpha}, I_{g-\beta}$ are the derived orthogonal signals of grid current.

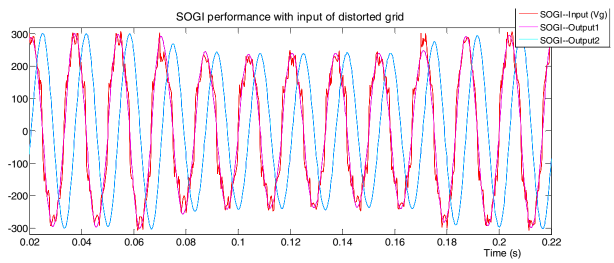

Fig.8(a) Grid voltage with 10%THD harmonics sags by 20% at 0.07s

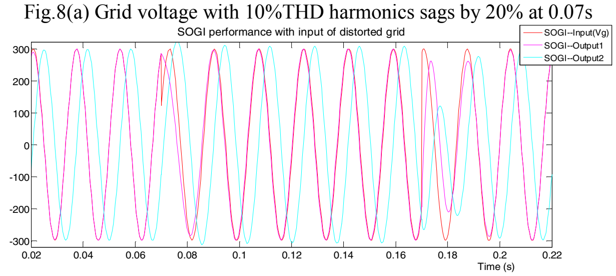

Fig.8(b).Grid frequency steps from 60Hz to 58Hz at 0.07s

IV. SIMULINK RESULTS

The simulation model based on Fig. 1 is built in MATLAB. The component parameters are listed in Table I.

Table I. MAIN PARAMETERS OF SIMULATION MODULE

Dc bus voltage	400 V	**Frequency of Grid voltage**	60 Hz
L1	6 mH	**L2**	1.2 mH
C	10 uF	**Rating of output Power**	500 W
Amplitude of Vg	300 V	**Switching frequency**	20 kHz

A. Performance under Various Distorted Grid Conditions

1) In this case, suppose the ideal grid is combined with 4% 3th, 4% 5th, 3% 7th and 3% 11th order harmonics beginning from 0.08 s and then resumes to the ideal condition without those harmonic component at 0.15 s, the corresponding system output performance can be seen in Fig. 9. The THD of I_g is as low as 2.49% under the distorted case.

2) In this case, suppose the grid voltage ($V_g = 300\ V$) sags by 10% suddenly at 0.08 s and then resumes to original condition at time 0.15 s, the output performance of system can be seen in Fig. 10. In this case, the proposed control method ensures the constant output power and perfect grid current even though the grid voltage sags. The THD of I_g is 1.01% in this case.

3) In this case, suppose the grid frequency step changes from 60 Hz to 58 Hz at 0.08 s and then resumes to the original condition at 0.15 s, the output performance of system can be seen in Fig. 11. In this case, the proposed control method can enforce grid current tracking grid frequency with constant output power even though grid frequency changes. And the THD of I_g is as low as 1.24% in this case.

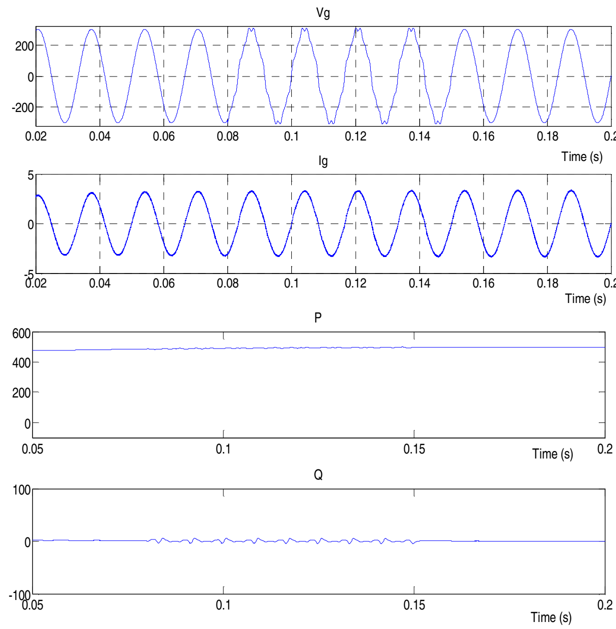

Fig.9. Output of system with grid with harmonics

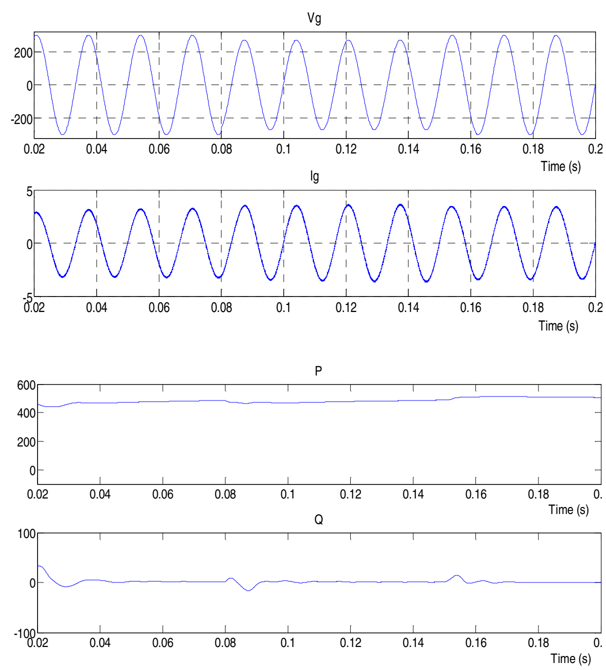

Fig.10. Output of system with grid voltage sag

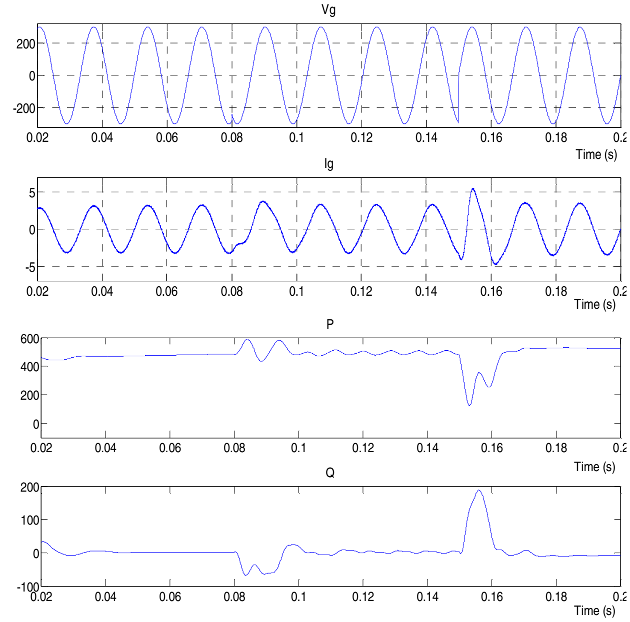

Fig.11. Output of system with grid frequency distortion

Decoupled Real and Reactive Power Control & Dynamic Performance

Suppose the reference value of real power and reactive power step change simultaneously at both 0.1s and 0.2s, the corresponding output performance of the system with given reference values is shown in Fig. 12

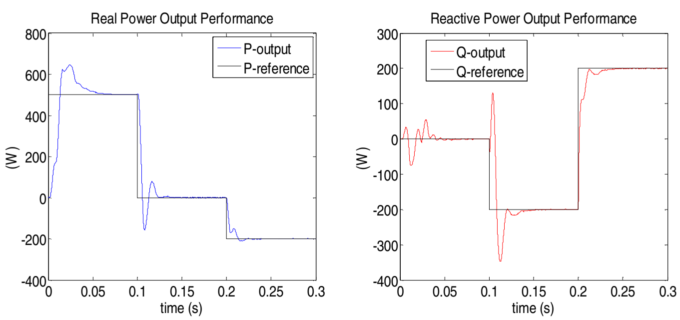

Fig.12 Step response of real and reactive power (Bidirectional)

As one can see from Fig. 12, the system keeps stable under different step-change conditions. And the output power of system is able to track the reference values well in less than 0.1 s, which proves a good dynamic performance. Moreover, the simulation results show that the real power and reactive power can be controlled separately and independently. And the controller reference values of power can be both negative and positive, which means the inverter system can not only support power as a source but also consume power as a load with flexible power factor.

V. Experimental Results

To verify above analysis, the proposed control strategy is implemented with dSPACE1007 with parameters in Table 1. Fig. 13(a) demonstrates the system performance under steady state condition, when the real power reference value is given as 500 W and reactive power reference value is given as 0 VA. In this case, the output grid current tracks the reference well with good waveform as shown in results.

The dynamic performance of the converter with the proposed scheme is presented in Fig. 13(b), where the real power reference value step changes from 500 W to 200 W at 0.1 s and reactive power reference value step changes from 300 VA to -300 VA at the same time with the change of real power reference value. These results show the decoupled power control ability of the proposed control strategy with good dynamic performance.

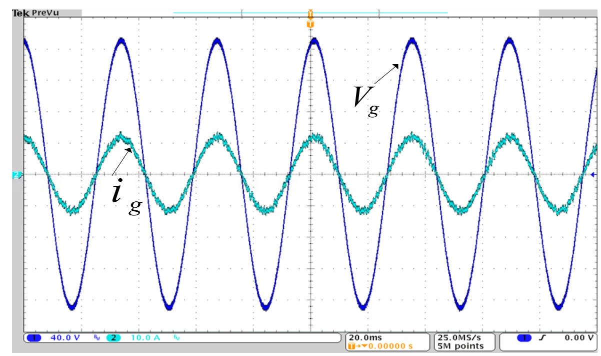

Fig. 13(a). Steady-state performance

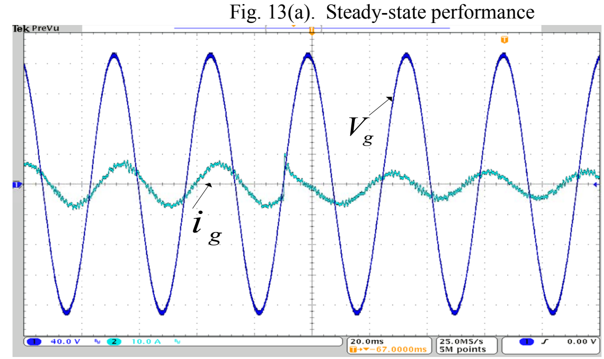

Fig. 13(b). Dynamic performance

VI. Conclusions

In this paper, a simplified and robust controller for single-phase grid connected inverter with LCL filter is proposed. The synchronization function is directly combined in power loop to replace the function of PLL. A double-loop current controller with PR compensator and active damping function is implemented to achieve better dynamic performance and larger stability range in this paper. Reliable performance under various grid distortion cases, high-quality output current and decoupled real and reactive power control abilities of inverter system are achieved in this way. The whole control system is implemented in stationary reference frame, which helps simplify the control algorithm.

VII. References

[1] R. I. Bojoi, L. R. Limongi, D. Roiu, and A. Tenconi, “Enhanced power quality control strategy for single-phase inverters in distributed generation systems,” IEEE Trans. Power Electron., vol. 26, no.3, pp. 798–806, Mar. 2011.

[2] S. Xu, J. Wang, and J. Xu, “A current decoupling parallel control strategy of single-phaseInverterwith voltage and current dual closed-loop feedback,” IEEE Trans. Ind. Electron., vol. 60, no. 4, pp. 1306–1313, Apr. 2013.

[3] P. Sun, C. Liu, J.-S. Lai, and C.-L. Chen, “Grid-tie control of cascade dualbuck inverter with wide-range power flow capability for renewable energy applications,” IEEE Trans. Power Electron., vol. 27, no. 4, pp. 1839–1849, Apr. 2012.

[4] B. Bahrani., et al., “Vector control of single-phase voltage source converters based on fictive-axis emulation,” IEEE Trans. Ind. Appl., vol. 47, no.2, pp. 831– 840, Mar. 2011

[5] Shadmand M B , Balog R S, Abu Rub H, “Maximum Power Point Tracking using Model Predictive Control of a flyback converter for photovoltaic applications,”Power and Energy Conference at Illinois (PECI), 2014. IEEE, 2014: 1-5.

[6] Shadmand M B, Mosa M, Balog R S, et al, “An improved MPPT technique for high gain DC-DC converter using model predictive control for photovoltaic applications,”Applied Power Electronics Conference and Exposition (APEC), 2014 Twenty-Ninth Annual IEEE. IEEE, 2014: 2993-2999.

[7] Q.-C. Zhong, et al., “Self-Synchronized Synchronverters: Inverters Without a Dedicated Synchronization Unit,” IEEE Trans. Power Electron., vol. 29, no. 2, pp. 617-630, Feb. 2014.

[8] S.-K. Chung, “A Phase Tracking System for Three Phase Utility Interface Inverters,” IEEE Trans. Power Electron., vol. 15, no. 3, pp. 431-438, May 2000.

[9] Q. Zhang, et al., “Analysis and Design of a Digital Phase-Locked Loop for Single-Phase Grid-Connected Power Conversion Systems,” IEEE Trans. Ind. Electron., vol.58,no.8, pp. 3581-3592, Aug. 2011.

[10] M. Rubens, et al., “Comparison of Three Single-Phase PLL Algorithms for UPS Applications,” IEEE. Trans. Ind. Electron., vol. 55, no. 8, pp. 2923-2931, Aug. 2008.

[11] Liu W, Hao X, Yang X, et al. A multi-resonant sliding-mode controller for single-phase grid-connected inverter with LCL-filter[C]//Applied Power Electronics Conference and Exposition (APEC), 2013 Twenty-Eighth Annual IEEE. IEEE, 2013: 2541-2546.

[12] Guofei T, Guochun X, Zhibo Z, et al. A control method with grid disturbances suppression for a single-phase LCL-filter-based grid-connected inverter[C]//Applied Power Electronics Conference and Exposition (APEC), 2012 Twenty-Seventh Annual IEEE. IEEE, 2012: 1489-1493.

[13] Cao B, Chang L. A variable switching frequency algorithm to improve the total efficiency of single-phase grid-connected inverters[C]//Applied Power Electronics Conference and Exposition (APEC), 2013 Twenty-Eighth Annual IEEE. IEEE, 2013: 2310-2315.

[14] Khajehoddin S A, Karimi-Gharteman M, Bakhshai A, et al. High quality output current control for single phase grid-connected inverters[C]//Applied Power Electronics Conference and Exposition (APEC), 2014 Twenty-Ninth Annual IEEE. IEEE, 2014: 1807-1814.